Activating mutations and translocations in the guanine exchange factor VAV1 in peripheral T-cell lymphomas

Francesco Abate[a,1], Ana C. da Silva-Almeida[b,1], Sakellarios Zairis[a], Javier Robles-Valero[c], Lucile Couronne[d,e,f], Hossein Khiabanian[a], S. Aidan Quinn[b], Mi-Yeon Kim[b], Maria Antonella Laginestra[g], Christine Kim[b], Danilo Fiore[h], Govind Bhagat[i], Miguel Angel Piris[j], Elias Campo[k], Izidore S. Lossos[l,m], Olivier A. Bernard[n,o,p], Giorgio Inghirami[h], Stefano Pileri[g], Xosé R. Bustelo[c,q], Raul Rabadan[a,r,2], Adolfo A. Ferrando[b,i,s,2], and Teresa Palomero[b,i,2]

[a]Department of Systems Biology, Columbia University Medical Center, New York, NY 10032; [b]Institute for Cancer Genetics, Columbia University, New York, NY 10032; [c]Centro de Investigación del Cáncer, Consejo Superior de Investigaciones Científicas-University of Salamanca, 37007 Salamanca, Spain; [d]Department of Adult Hematology, Necker Hospital, 75015 Paris, France; [e]INSERM UMR163, Centre National de la Recherche Scientifique Équipe de Recherche Labellisée 8254, Institut Imagine, 75015 Paris, France; [f]Paris Descartes University, 75006 Paris, France; [g]Hemopathology Unit, European Institute of Oncology, 20139 Milan, Italy; [h]Department of Pathology and Laboratory Medicine, Weill Cornell Medical College, New York, NY 10065; [i]Department of Pathology and Cell Biology, Columbia University Medical Center, New York, NY 10032; [j]Instituto de Formación e Investigación, Hospital Universitario Marqués de Valdecilla, 39008 Santander, Spain; [k]Department of Pathology, Hospital Clinic, 08036 Barcelona, Spain; [l]Division of Hematology-Oncology, Sylvester Comprehensive Cancer Center, Miami, FL 33136; [m]Department of Molecular and Cellular Pharmacology, University of Miami, Miami, FL 33101; [n]INSERM U1170, 94805 Villejuif, France; [o]Université Paris-Sud, 91405 Orsay, France; [p]Gustave Roussy, 94805 Villejuif, France; [q]Centro de Investigacion Biomedica en Red de Cancer (CIBERONC), Spain; [r]Department of Biomedical Informatics, Columbia University Medical Center, New York, NY 10032; and [s]Department of Pediatrics, Columbia University Medical Center, New York, NY 10032

Edited by Seishi Ogawa, Kyoto University, Kyoto, Japan, and accepted by Editorial Board Member Tadatsugu Taniguchi December 5, 2016 (received for review June 3, 2016)

Peripheral T-cell lymphomas (PTCLs) are a heterogeneous group of non-Hodgkin lymphomas frequently associated with poor prognosis and for which genetic mechanisms of transformation remain incompletely understood. Using RNA sequencing and targeted sequencing, here we identify a recurrent in-frame deletion (VAV1 Δ778–786) generated by a focal deletion-driven alternative splicing mechanism as well as novel *VAV1* gene fusions (*VAV1-THAP4*, *VAV1-MYO1F*, and *VAV1-S100A7*) in PTCL. Mechanistically these genetic lesions result in increased activation of VAV1 catalytic-dependent (MAPK, JNK) and non–catalytic-dependent (nuclear factor of activated T cells, NFAT) VAV1 effector pathways. These results support a driver oncogenic role for VAV1 signaling in the pathogenesis of PTCL.

peripheral T-cell lymphoma | VAV1 | mutation | gene fusion

Peripheral T-cell lymphomas (PTCLs) are malignant and highly aggressive hematologic tumors arising from mature postthymic T cells (1). The diagnosis of PTCL includes diverse lymphoma subgroups, altogether accounting for about 15% of all non-Hodgkin lymphomas (2, 3). Despite much effort in developing reliable diagnostic markers, the diagnosis of PTCLs is challenging, and 20 to 30% of cases are diagnosed as PTCL-NOS (not otherwise specified). This heterogeneous and poorly defined group constitutes one of the most aggressive forms of non-Hodgkin lymphoma, in which limited response to intensified chemotherapy and high relapse rates result in a dismal 5-y overall survival rate of 20 to 30% (4, 5). Moreover, a paucity of information on driver oncogenes activated in PTCL-NOS hampers the development of targeted therapies in this aggressive lymphoma subgroup.

The *VAV1* protooncogene encodes a guanine nucleotide exchange factor (GEF) and adaptor protein with crucial signaling roles in protein tyrosine kinase-regulated pathways (6). Structurally, VAV1 contains a calponin homology domain and an acidic domain in the N terminus followed by a GEF catalytic active core consisting of a central Dbl homology domain, pleckstrin homology domain, and C1 domain (6). Finally, the C-terminal region of VAV1 contains three Src homology domains in an SH3-SH2-SH3 arrangement (6). The GEF activity of VAV1 stimulates the transition of RAC1 and RHOA small GTPases from their inactive (GDP-bound) to the active (GTP-bound) configuration (6–8). In addition, the adaptor function of VAV1 mediates activation of the nuclear factor of activated T cells (NFAT) in synergy with signals from antigenic receptors in lymphoid cells (6, 8–13). In basal conditions, unphosphorylated VAV1 adopts an inactive closed configuration in which the N-terminal calponin homology and acidic domains and the C-terminal SH3 (C-SH3) domain block access of small GTPases to the catalytic core and limit the noncatalytic activities of the protein (6, 14, 15). Activation of VAV1 by transmembrane and cytosolic protein kinases reverses these intramolecular inhibitory interactions by promoting an open active configuration associated with phosphorylation in the acidic, C1 finger, and C-SH3 domains (6, 14, 15).

VAV1 is specifically expressed in hematopoietic tissues, and plays key roles in lymphocyte development and function (8). VAV1 is essential for T-cell receptor (TCR)-mediated cytoskeletal reorganization, cytokine secretion, proliferation, and survival (8, 12). Thus, *Vav1*-deficient mice show a partial block in thymic development at the $CD4^-$ $CD8^-$ double-negative to $CD4^+$ $CD8^+$ double-positive transition, defective positive selection, and impaired negative selection, which altogether point to a major role for VAV1 in TCR signaling (16, 17). Biochemically, mouse *Vav1* knockout T cells fail to elicit TCR-induced intracellular Ca^{2+} flux and to activate MAP/ERK pathway and NF-κB signaling (18–21). Consistently, the function of mature T-cell populations is also defective in the absence of Vav1, with reduced TCR-induced

Significance

Guanine nucleotide exchange factor *VAV1* encodes an adaptor and signal transduction factor with important roles in T-cell receptor signaling. This study identifies activating *VAV1* recurrent mutations and *VAV1* fusions in peripheral T-cell lymphomas, directly establishing an oncogenic role for constitutive VAV1 signaling in the pathogenesis of this disease.

Author contributions: H.K., X.R.B., R.R., A.A.F., and T.P. designed research; A.C.d.S.-A., J.R.-V., L.C., M.-Y.K., C.K., and T.P. performed research; M.A.L., D.F., G.B., M.A.P., E.C., I.S.L., O.A.B., G.I., and S.P. contributed new reagents/analytic tools; F.A., A.C.d.S.-A., S.Z., H.K., S.A.Q., X.R.B., R.R., A.A.F., and T.P. analyzed data; and A.A.F. and T.P. wrote the paper.

The authors declare no conflict of interest.

This article is a PNAS Direct Submission. S.O. is a Guest Editor invited by the Editorial Board.

Data deposition: The next-generation sequencing data reported in this paper have been deposited in the database of Genotypes and Phenotypes (dbGaP), https://www.ncbi.nlm.nih.gov/ (accession no. phs000689.v1.p1) and the Sequence Read Archive at the National Center for Biotechnology Information, https://www.ncbi.nlm.nih.gov/sra/ (accession nos. SRP029591, PRJNA255877, and SRP057085).

[1]F.A. and A.C.d.S.-A. contributed equally to this work.

[2]To whom correspondence may be addressed. Email: rr2579@cumc.columbia.edu, af2196@columbia.edu, or tp2151@columbia.edu.

This article contains supporting information online at www.pnas.org/lookup/suppl/doi:10.1073/pnas.1608839114/-/DCSupplemental.

proliferation and cytokine secretion (8, 22, 23). Similarly, VAV1-null human JURKAT T cells show impaired TCR-induced calcium flux, IL-2 transcription, and NF-κB activation, as well as decreased TCR-induced JNK and NFAT signaling (24).

Here we report the identification and functional characterization of recurrent activating mutations and gene fusions in *VAV1* in PTCL.

Results

Identification of *VAV1* Mutations and Gene Fusions in PTCL. To identify new genetic drivers responsible for T-cell transformation and potential targets for therapy in PTCL, we performed a systematic analysis of genetic alterations using RNA-sequencing (RNA-seq) data from a cohort of 154 PTCL samples, including 41 PTCL-NOS, 60 angioimmunoblastic T-cell lymphoma (AITL), 17 natural killer/T-cell lymphoma (NKTCL), and 36 anaplastic large T-cell lymphoma (ALCL) tumors (25–27) (Dataset S1). These analyses confirmed a high prevalence of *RHOA*, *TET2*, *IDH2*, and *DNMT3A* mutations in AITL (25, 26, 28) and the recurrent presence of fusion transcripts involving the *ALK1* gene, including *NPM1-ALK1*, *TRAF1-ALK*, and *TPM3-ALK*, and *STAT3* activating mutations in ALCL (27) (*SI Appendix*, Fig. S1 and Dataset S2). However, the most notable finding of these analyses was the identification of gene fusions and novel recurrent mutations involving the *VAV1* protooncogene. Specifically, we identified three different fusion transcripts encoding proteins in which the C-terminal SH3 domain of VAV1 is replaced by the calycin-like domain of THAP4 (in two cases), the SH3 domain of MYO1F, or the EF domains of S100A7 (Fig. 1, *SI Appendix*, Figs. S1 and S2, and Dataset S3). Reverse-transcription PCR amplification and DNA sequencing validated the expression of each of these *VAV1* chimeric mRNAs in all samples analyzed (Fig. 1). In addition, we identified two PTCL cases harboring a novel intragenic *VAV1* in-frame deletion, r.2473_2499del, which results in the loss of nine amino acids (p.Val778_Thr786del) in the linker region between the SH2 and C-terminal SH3 domains of the VAV1 protein (Fig. 2 and *SI Appendix*, Figs. S3 and S4).

To further explore the prevalence and mechanisms of *VAV1* mutations in PTCL, we performed targeted genomic DNA sequencing of *VAV1* in a panel of 126 PTCL samples. Genomic DNA sequencing of the two index RNA-seq cases harboring the r.2473_2499del mutation revealed the presence of focal genomic deletions in *VAV1* involving the 3′ end of intron 25 and extending into exon 26 (g.81269_81294del and g.81275_81302del) (Figs. 2*B* and 3*A* and *SI Appendix*, Fig. S4). In addition, we identified additional three cases harboring similar focal genomic deletions involving the *VAV1* intron 25–exon 26 boundary (g.81275_81301del, g.81279_81296indelA, and g.81279_81298del) and one additional case with a mutation resulting in the loss of 19 nt at the 5′ end of exon 26 but preserving the intron 25–exon 26 AG splice acceptor sequence (g.81280_81298indelA) (Figs. 2*B* and 3*A* and *SI Appendix*, Fig. S4). cDNA-sequencing analysis in three of our additional mutated cases for which RNA was available, including case PTCL CU44, in which the deletion spared the canonical exon 26 splice acceptor site, revealed that in all cases these mutations resulted in activation of a cryptic splice acceptor site in exon 26 and the consequent expression of missplicied transcripts containing the r.2473_2499del (p.Val778_Thr786del) *VAV1* mutation (Fig. 2*B*). Notably, analysis of *VAV1* exon 26 sequences proximal to this cryptic splice acceptor site uncovered the presence of an exonic splicing silencer element (29), which is disrupted or completely lost in all *VAV1* intron 25–exon 26 indel mutated cases analyzed (Fig. 3). Altogether, PTCL *VAV1* intron 25–exon 26 deletions activate a cryptic *VAV1* exon 26 splice acceptor site by disrupting the corresponding intron 25–exon 26 canonical splice acceptor sequence (5/6 cases) and removing an exon 26 exonic splicing silencer (6/6 cases). In addition to removing these splicing regulatory elements, these focal deletions reconfigure the architecture

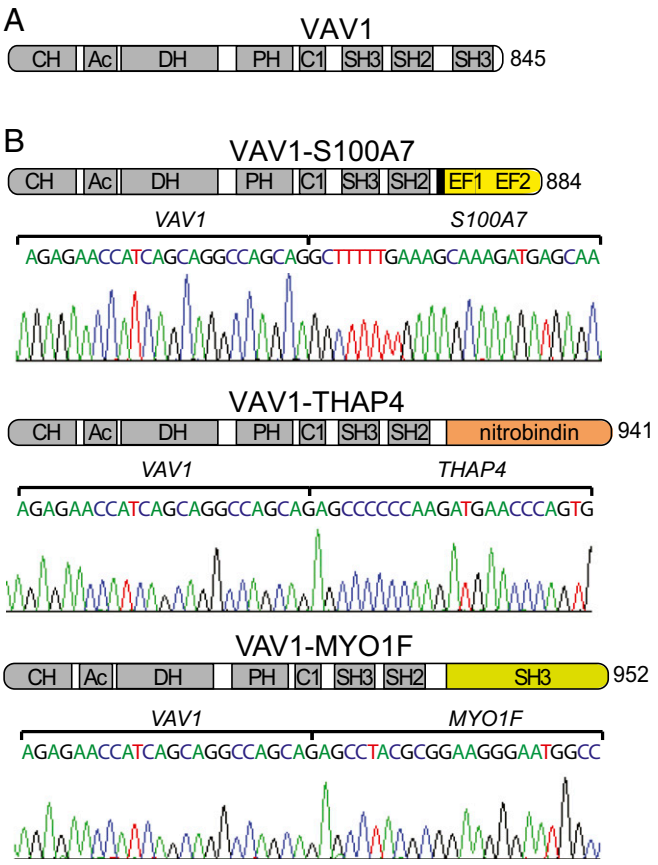

Fig. 1. *VAV1* fusion genes in PTCL. (*A*) Schematic representation of the domain structure of the VAV1 protein. (*B*) Schematic representation of the domain structures of the VAV1-S100A7, VAV1-THAP4, and VAV1-MYO1F fusion proteins. Ac, acidic domain; C1, C1 domain; recognition motif for diacylglycerol and phorbol esters, atypical; CH, calponin homology domain; DH, DBL homology; EF, pseudo-EF hand domain; nitrobindin, nitrobindin domain; PH, pleckstrin homology domain; SH2, Src homology 2 domain; SH3, Src homology 3 domain.

of the intron 25–exon 26 boundary by placing the intron 25 polypyrimidine tract immediately distal to the alternative exon 26 AG splice acceptor site (6/6 cases) (Fig. 3 *C* and *D*). Additionally, our mutation analyses also identified three nonrecurrent point mutations resulting in amino acid substitutions in the Dbl homology (p.His337Tyr), C1 finger (p.Glu556Asp), and C-terminal SH3 domains (p.Arg798Pro) of VAV1 (*SI Appendix*, Figs. S1 and S5 and Datasets S2 and S4).

VAV1 Fusion Proteins Induce Increased VAV1 Signaling. Given the prominent role of VAV1 in T-cell activation and to explore the functional consequences of PTCL-associated *VAV1* mutations and gene fusions, we analyzed the effect of these genetic alterations on lymphocyte signaling. Recent reports have demonstrated that the C-terminal SH3 domain of VAV1 contributes to intramolecular inhibition of VAV protein family members (14). Considering that our fusions and intragenic deletion mutants specifically affect the region containing the C-SH3 domain of the protein, we used the VAV1 Δ835–845 deletion mutant, which lacks the C-SH3 domain, as positive control in our experiments. To avoid interference with endogenous VAV1, JURKAT cells lacking endogenous expression of VAV1 protein (Jurkat J.VAV1) were infected with lentiviral constructs for *VAV1* Δ778–786 and the *VAV1-MYO1F*, *VAV1-S100A7*, and *VAV1-THAP4* fusions as well as the empty vector, *VAV1* wild type, and *VAV1* Δ835–845 controls. Analysis of signaling events downstream of VAV1 demonstrated

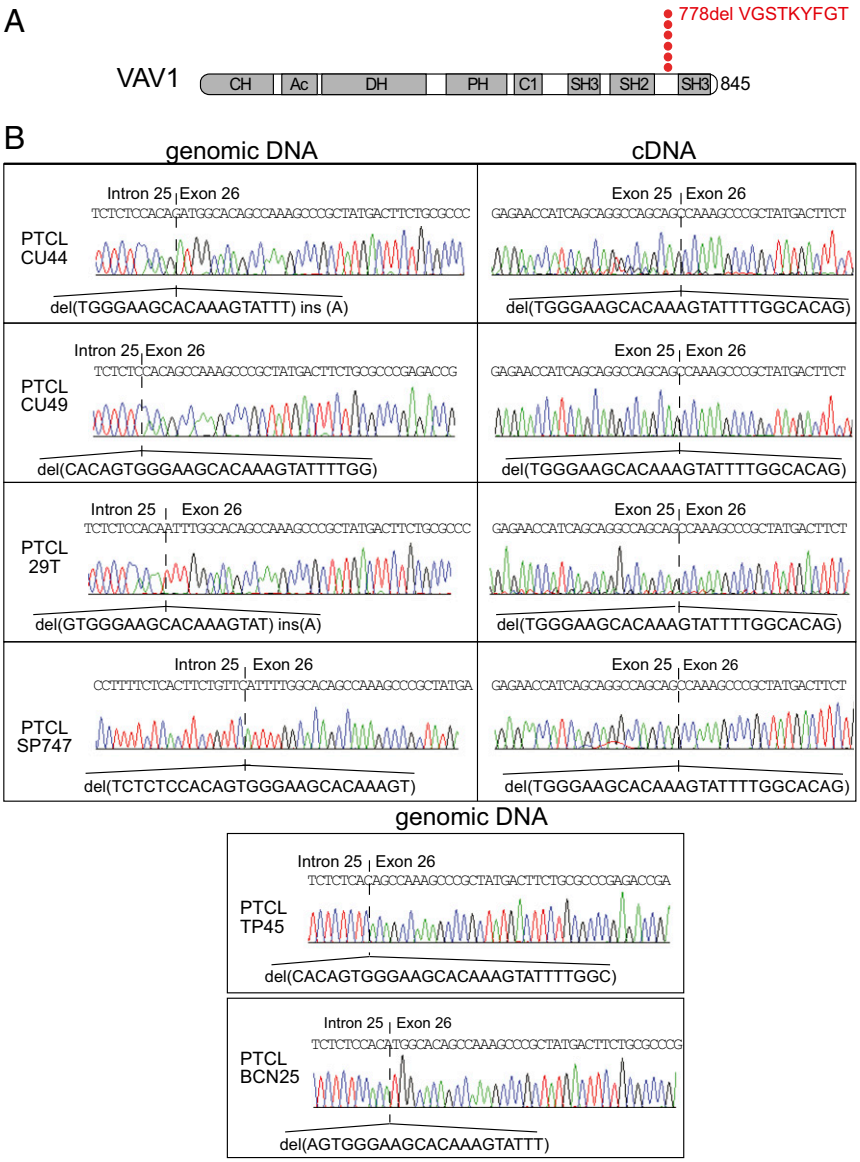

Fig. 2. Recurrent VAV1 Δ778–786 mutation in PTCL. (*A*) Schematic representation of the domain structure of the VAV1 protein indicating the location of the VAV1 p.778delVGSTKYFGT (VAV1 Δ778–786) mutation. Each red circle is indicative of a PTCL mutant sample. (*B*) Genomic DNA and cDNA sequences corresponding to the intron 25–exon 26 genomic DNA and exon 25–exon 26 cDNA boundaries, respectively, in PTCL samples harboring the VAV1 p.778delVGSTKYFGT (VAV1 Δ778–786) mutation.

increased phosphorylation in ERK1/2 but not in PLCγ1 in JURKAT J.Vav1 cells expressing VAV1 Δ778–786, and the VAV1-MYO1F, VAV1-S100A7, and VAV1-THAP4 fusions, compared with wild-type VAV1 (Fig. 4*A*). Additionally, we also analyzed the impact of the p.His337Tyr, p.Glu556Asp, and p.Arg798Pro missense mutations identified in our study, as well as that of p.E157Lys, p.Lys404Arg, p.Gln498Lys, and p.Met501Arg VAV1 missense mutations identified in adult T-cell lymphoma (ATL) (4), on the phosphorylation and activation of signaling pathways downstream of VAV1 (*SI Appendix*, Fig. S5). These analyses revealed weaker and variable effects of these mutations, with only VAV1 p.Gln498Lys showing clear increased ERK1/2 phosphorylation and modestly higher levels of phospho-PLCγ1 (*SI Appendix*, Fig. S5).

Analysis of JNK signaling in AP1 reporter assays, a functional readout of VAV1 catalytic-dependent functions downstream of RAC1, showed marked increased JNK activation in JURKAT cells expressing the VAV1-MYO1F, VAV1-S100A7, and VAV1-THAP4 fusions (Fig. 4*B*). Notably, this effect was primarily independent of TCR stimulation with anti-CD3 supporting that PTCL-associated VAV1 fusion proteins adopt a constitutively active configuration. In contrast, expression of the VAV1 Δ778–786 mutant protein induced only minor increases in JNK activation compared with wild-type VAV1, even after anti-CD3 stimulation (Fig. 4*B*). Next, and to explore noncatalytic VAV1 activity, we analyzed the effects of VAV1 Δ778–786 mutant and fusion proteins in NFAT reporter assays in JURKAT cells (Fig. 4*C*). In these experiments, expression of VAV1-MYO1F, VAV1-S100A7, and VAV1-THAP4 fusions induced increased NFAT activity, which was further increased upon anti-CD3 stimulation (Fig. 4*C*). In contrast, VAV1 Δ778–786 expression induced NFAT responses similar to those elicited by expression of wild-type VAV1 (Fig. 4*C*). Consistently, VAV1-MYO1F, VAV1-S100A7, and VAV1-THAP4 fusions strongly increased transcription of *CD40L* and *IL-2* NFAT target genes, in basal conditions and after stimulation with anti-CD3 in JURKAT J.VAV1 cells, whereas expression of VAV1 Δ778–786 resulted in only a modest increase in gene expression (Fig. 4*D*).

VAV1 Δ778–786 and VAV1 Fusions Induce an Open Active VAV1 Configuration. The inhibitory role of VAV1 C-terminal SH3 domain involves its folding over to the N-terminal catalytic and pleckstrin homology domains, which occludes the access of VAV effector factors to the catalytic GEF domain (14). Thus, we postulated that the loss of the C-terminal SH3 domain in the

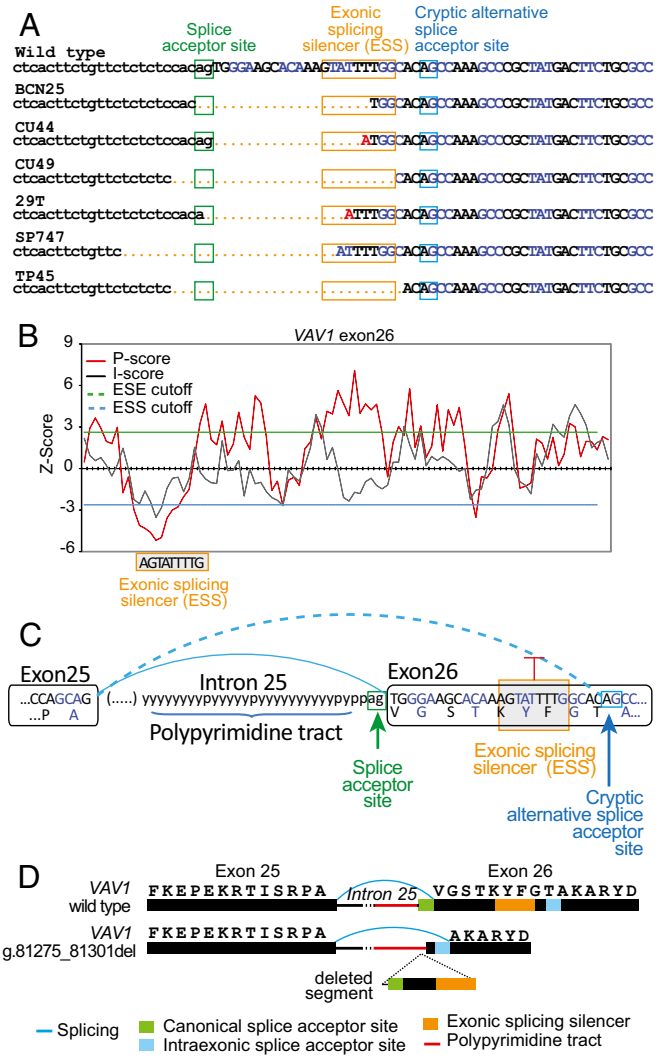

Fig. 3. *VAV1* intron 25–exon 26 deletion–induced missplicing and VAV1 Δ778–786 expression. (*A*) Genomic DNA sequences for PTCLs with verified intron 25–exon 26 indel mutations. Deleted genomic DNA sequences are indicated with orange dotted lines. Inserted nucleotides are indicated in red. Intron 25 nucleotides are shown in lowercase letters. Exon 26 nucleotides are indicated in capital letters. (*B*) *VAV1* exon 26 splicing sequencer analysis. ESE, exonic splicing enhancer; ESS, exonic splicing silencer. *P* scores indicate the *Z* value for sequence over/underrepresentation in internal noncoding exons vs. pseudo exons. *I* scores indicate the *Z* value for sequence over/underrepresentation in internal noncoding exons vs. 5′ UTRs of intronless genes. Underrepresented octamers are assigned negative *Z* scores. Nine nucleotides corresponding to two overlapping octamers, GTATTTAT and TATTTATG, with strong exonic splicing silencer scores are boxed in orange. (*C*) Scheme of genomic DNA of wild-type *VAV1* intron 25–exon 26 boundary indicating the intron 25 polypyrimidine tract and splice acceptor sequence (green box), exon 26 exonic splicing silencer (orange box), and the cryptic alternative splice acceptor site activated in PTCL samples harboring *VAV1* intron 25–exon 26 indel mutations (blue box). Partial sequences of exons 25 and 26 (capital letters) and intron 25 (lowercase letters) are shown. (*D*) Schematic representation of a representative *VAV1* intron 25–exon 26 mutation (g.81275_81301del) and the consequent missplicing-induced deletion (r.2473_2499del) and protein product (p.Val778_Thr786del; VAV1 Δ835–845).

VAV1-MYO1F, VAV1-S100A7, and VAV1-THAP4 fusions would result in VAV1 activation via loss of these inhibitory intramolecular interactions. Moreover, we proposed that the removal of nine amino acids proximal to the C-terminal SH3 domain in the VAV1 Δ778–786 mutant protein could also limit the inhibitory role of this domain by favoring an open VAV1 conformation. To test this hypothesis, we analyzed the levels of Tyr174 phosphorylation, a regulatory posttranslational modification indicative of an active VAV1 open configuration (7, 15), in VAV1 wild type, VAV1 Δ835–845, VAV1 Δ778–786, and the VAV1-MYO1F, VAV1-S100A7, and VAV1-THAP4 fusions or control empty vector. Consistent with the loss of the inhibitory role of the VAV1 C-terminal SH3 domain, immunoprecipitation of HA-tagged VAV1 proteins with anti-HA antibody in these cells, followed by immunoblotting with an antibody recognizing phospho-Y174, showed high levels of phosphorylation in VAV1-MYO1F, VAV1-S100A7, and VAV1-THAP4 fusions (Fig. 4*E*). Similarly, we also observed increased levels of VAV1 Y174 phosphorylation in the VAV1 Δ778–786 mutant protein (Fig. 4*E*) compared with VAV1 wild-type controls. These results support that the PTCL-associated VAV1 Δ778–786 mutation and in particular the VAV1-MYO1F, VAV1-S100A7, and VAV1-THAP4 fusion proteins can adopt an open configuration even in the absence of TCR stimulation and mechanistically implicate the loss or impairment of the inhibitory role of the C-terminal SH3 domain of VAV1 in the pathogenesis of PTCL (Fig. 4*E*). Similar results were also obtained in HEK293T cells in the context of VAV1 signaling activated by FYN kinase expression (*SI Appendix*, Fig. S6).

Discussion

Initially identified as a protooncogene isolated in a gene transfer screen for oncogenes with the ability to transform NIH 3T3 fibroblasts (30), the oncogenic activity of the original VAV1 clone resulted from an artificially generated N-terminal deletion driving increased VAV1 activation (31). A pathogenic role for the VAV family of signaling factors in cancer has been proposed primarily based on their deregulated expression in solid tumors and hematological malignancies (32). In addition, recent genomic profiling analyses of ATL have revealed the presence of recurrent point mutations in *VAV1* in this disease (33), and *VAV1* gene fusions have recently been implicated in one case of ATL and more broadly in PTCL (34). *VAV1* mutations identified in ATL result mostly in single-amino acid substitutions involving the acidic, pleckstrin homology, C1 finger, and C-terminal SH3 domains of the VAV1 protein (33). In addition, both the VAV1 gene fusion found in ATL (VAV1-TRIP10) (33) and those reported in two cases of PTCL-NOS (VAV1-MYO1F and VAV1-GSS) (34) involve the loss of the C-terminal SH3 domains of VAV1. The recurrent pattern of *VAV1* mutations and gene fusions found in PTCL (34) and ATL (33) support a gain-of-function mechanism. Moreover, the identification here of additional *VAV1* genetic alterations in PTCL, including a novel recurrent in-frame deletion resulting in the loss of amino acids 778–786 in the linker region between the SH2 and C-terminal SH3 domains of VAV1, further supports a pathogenic role for VAV1 signaling in T-cell transformation. However, constitutive genetic loss of *Vav1* is associated with the development of aggressive T-cell lymphoblastic lymphomas in aged mice (35, 36), probably as a result of deregulated oncogenic pathways activated in response to defective Vav1 signaling (37).

Functional characterization of PTCL-associated VAV1 fusion proteins revealed increased levels of VAV1 activation, implicating the loss of C-terminal SH3 domain-mediated VAV1 regulation in PTCL transformation. In this context, it is worth noting that an artificially generated VAV1 mutant protein devoid of the C-terminal SH3 domain, VAV1 Δ835–845, shows increased VAV1 signaling (14). Moreover, the recurrent *VAV1* Δ778–786 mutation and PTCL- and ATL-associated *VAV1* missense mutations analyzed here also behaved as a gain-of-function allele, eliciting increased levels of VAV1 effector pathway activation. However, no C-terminal protein-truncating mutations in *VAV1* were identified in our patient cohort, suggesting a role for the MYO1F, S100A7, and THAP4 domains fused to VAV1 in the oncogenic activity of VAV1-MYO1F, VAV1-S100A7, and VAV1-THAP4, respectively.

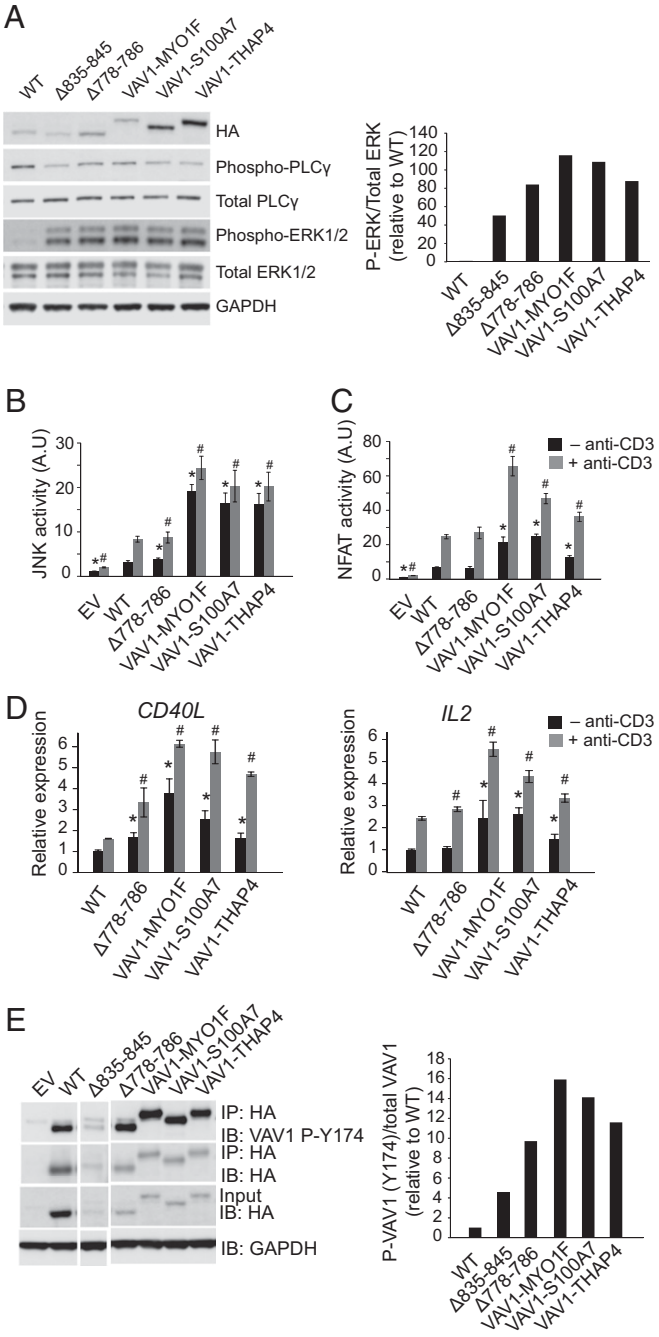

Fig. 4. VAV1 fusions and the VAV1 Δ778–786 mutation induce increased VAV1 signaling in T cells. (*A*) Analysis of ERK1/2 and PLCγ1 phosphorylation in J.VAV1 cells upon expression of VAV1 fusion proteins or the VAV1 Δ778–786 intragenic deletion mutant. The VAV1 Δ835–845 C-terminal SH3 domain deletion mutant is used as positive control for VAV1 activity. (*B* and *C*) Reporter assays analyzing JNK (*B*) and NFAT activity (*C*) in JURKAT cells expressing wild-type, mutant, or fusion VAV1 proteins in basal conditions and upon stimulation with anti-CD3. A.U., arbitrary units. (*D*) Quantitative RT-PCR analysis of *CD40L* and *IL2* NFAT target genes in JURKAT cells expressing wild-type, mutant, or fusion VAV1 proteins in basal conditions and upon stimulation with anti-CD3. (*E*) Immunoprecipitation/Western blot analysis of VAV1 Tyr174 phosphorylation in J.VAV1 cells upon expression of wild-type and mutant or fusion VAV1 proteins shows increased activated phosphorylation of VAV1 mutants and fusion proteins compared with wild-type control. Bar graphs in *B*–*D* show mean values, and error bars represent the SD. Values are indicative of results in triplicate samples in a representative example of three independent experiments. *P* values were calculated using two-tailed Student's *t* test; $^{*}P < 0.05$ relative to nonstimulated wild-type VAV1-expressing cells; $^{\#}P < 0.05$ relative to stimulated wild-type VAV1-expressing cells. EV, empty vector; IB, immunoblotting; IP, immunoprecipitation.

In VAV1-S100A7, the C-terminal SH3 domain of VAV1 is replaced by the full length of S100A7, a calcium-binding epidermal protein with proposed antibacterial and chemoattractant roles (38). More interestingly, the *VAV1-MYO1F* fusion replaces the C-terminal SH3 domain of VAV1 by the also C-terminally located SH3 domain of *MYO1F*, an actin-interacting motor protein (39). Remarkably, a recent report identified an additional VAV1-MYO1F fusion in a PTCL sample (34), which further supports a possible role of the MYO1F SH3 domain in promoting the activity of the VAV1-MYO1F oncoprotein. Finally, the *VAV1-THAP4* fusion replaces the C-terminal SH3 domain of VAV1 with the C-terminal nitrobindin domain of THAP4 (40). The recurrent finding of the VAV1-THAP4 fusion in two independent samples in our cohort supports that, in addition to removing the C-terminal SH3 domain on VAV1, the incorporation of the β-barrel heme-Fe(III)–binding nitrobindin domain of THPA4 may play an active role in the activity of the VAV1-THAP4 oncoprotein. Animal models with selective expression of *VAV1* mutations and gene fusions will facilitate the analysis of the specific oncogenic roles and mechanisms of these genetic alterations in T-cell transformation.

The apparent predominance of *VAV1* point mutations in ATL compared with the more frequent occurrence of gene fusions and focal indel mutations in PTCL-NOS may be reflecting different mutagenic mechanisms or, alternatively, context-relevant specific functions of the resulting VAV1 oncoproteins in these diseases. Of note, the VAV1 Δ778–786 mutation involves a unique mechanism that couples genomic disruption of the *VAV1* intron 25–exon 26 boundary with a new splicing event triggered by the coordinated loss of an intraexonic splice silencer in exon 26 and the disruption of the canonical AG intron 25–exon 26 splice acceptor site. Somatic mutations involving splicing sites are a common mechanism of tumor suppressor gene inactivation in cancer, where disruption of splicing donor and acceptor site sequences frequently results in intron retention or exon skipping events and expression of aberrant transcripts containing premature stop codons (41). However, missplicing mutations can also result in oncogene activation. Thus, splicing site mutations in the *MET* oncogene promote exon 14 skipping and consequent expression of mutant oncogenic forms of MET with increased stability and prolonged signaling upon HGF stimulation (42). Similarly, mutations driving missplicing of the distal coding region of NOTCH1 into the 3′ UTR of this gene result in expression of C-terminally truncated forms of NOTCH1 with increased stability and prolonged signaling in chronic lymphocytic leukemia (43). In the case of VAV1 Δ778–786, an in-frame missplicing of exon 25 into a cryptic intraexonic splice acceptor motif in exon 26 generates mRNAs with an in-frame deletion and the expression of a gain-of-function VAV1 oncoprotein. These findings call for careful interpretation of the functional consequences of cancer-associated splice site mutations in genomic studies.

In all, our identification of recurrent activating events affecting *VAV1* in PTCL-NOS and AITL supports an important driver role for druggable effector signaling pathways downstream of VAV1 in T-cell transformation. These results warrant the comprehensive evaluation of the prevalence and clinical impact of *VAV1* genetic alterations on extended cohorts of homogeneously treated PTCL patients.

Materials and Methods

DNA and RNA samples from PTCL biopsies were obtained with informed consent in a multiinstitutional setting. Studies were conducted under the supervision of the Columbia University Medical Center Institutional Review Board.

Genomic Analyses. Mutational analysis of *VAV1* was performed by targeted resequencing using microfluidics PCR (Access Array System; Fluidigm) followed by sequencing of amplicon libraries in a MiSeq instrument (Illumina). We identified variants that differed from the reference genome using the SAVI algorithm (statistical algorithm for variant identification) based on coverage

depth and frequency (44). Candidate variants were independently validated by targeted deep sequencing. We analyzed Illumina HiSeq paired-end RNA-seq data from 154 PTCL samples and identified variants using GATK HaplotypeCaller (45) and Bcftools v1.2 (46) with standard parameters, and gene fusions using the ChimeraScan algorithm (47) and the Pegasus pipeline (48).

In Vitro Studies. We performed Western blot detection using standard procedures with the following antibodies: HA (Roche; 11867423001; 1:500), Vav1 phospho-Y174 (Abcam; ab76225; 1:1,000), Vav1 DH domain (49) (1:10,000 dilution), GAPDH (Cell Signaling Technology; 5174; 1:5,000), ERK (Santa Cruz Biotechnology; SC-271270; 1:250), phospho-p44/p42 (Cell Signaling Technologies; 4377; 1:1,000), PLC gamma1 (E-12) (Santa Cruz Biotechnology; SC-7290; 1:250), phospho-PLC gamma1 (Tyr783) (Cell Signaling Technologies; 2821; 1:1,000), and α-tubulin (Calbiochem; CP06; 1:2,000). We ran immunoprecipitation analyses on cleared cell lysates using EZview Red Anti-HA Affinity Gel (Sigma; E6779) and analyzed them by SDS/PAGE and immunoblotting.

For NFAT and JNK activation assays, we coelectroporated JURKAT cells with JUN (pFR-Luc, pFA2-c-Jun) or NFAT (pNFAT-luc, pRL-SV40) luciferase reporter vectors together with *VAV1* wild type or mutant expression constructs plus a *Renilla* luciferase internal normalization control.

We induced TCR stimulation with antibodies against human CD3 (Calbiochem; 217570; UCHT1 clone) and determined luciferase activity with the Dual-Luciferase Assay System (Promega).

Statistical Analyses. Analyses of significance were performed using Student's *t* test assuming equal variance. Continuous biological variables were assumed to follow a normal distribution. A P value of <0.05 was considered to indicate statistical significance.

Detailed information regarding the reagent assembly and assay conditions can be found in *SI Appendix, Materials and Methods*.

ACKNOWLEDGMENTS. This work was supported by National Cancer Institute R01 CA197945-01 (to T.P.), Leukemia & Lymphoma Society (LLS) Awards TRP-6507-17 (to T.P.) and TRP-6163-12 (to A.A.F.), a Herbert Irving Comprehensive Cancer Center interprogrammatic pilot project grant (to A.A.F. and R.R.), and Grant 10007 from the Italian Association for Cancer Research (AIRC) (to S.P.). O.A.B. was supported by Institut National du Cancer (INCa), 2013-1-PL BIO-09, INCa-DGOS-INSERM 6043, equipe labellisée Ligue Nationale Contre le Cancer (LNCC), and INCa-DGOS-INSERM 6043. X.R.B.'s work was supported by grants from the Spanish Ministry of Economy and Competitiveness (RD12/0036/0002, SAF2012-31371, and SAF2015-64556-R), Worldwide Cancer Research (14-1248), and Ramón Areces Foundation. A.C.d.S.-A. was supported by a Lady Tata Memorial Trust fellowship and an LLS Special Fellowship Award. S.Z. was supported by a TL1 personalized medicine fellowship (5TL1TR000082). L.C. was funded by a postdoctoral grant from Institut Multi Organismes Cancer and INCa. M.-Y.K. was funded by an LLS postdoctoral fellowship.

1. de Leval L, Gaulard P (2011) Pathology and biology of peripheral T-cell lymphomas. *Histopathology* 58(1):49–68.
2. Rüdiger T, Müller-Hermelink HK (2002) [WHO-classification of malignant lymphomas]. *Radiologe* 42(12):936–942. German.
3. Armitage JO (2015) The aggressive peripheral T-cell lymphomas: 2015. *Am J Hematol* 90(7):665–673.
4. Savage KJ, Ferreri AJ, Zinzani PL, Pileri SA (2011) Peripheral T-cell lymphoma—Not otherwise specified. *Crit Rev Oncol Hematol* 79(3):321–329.
5. Federico M, et al. (2013) Clinicopathologic characteristics of angioimmunoblastic T-cell lymphoma: Analysis of the International Peripheral T-Cell Lymphoma Project. *J Clin Oncol* 31(2):240–246.
6. Bustelo XR (2014) Vav family exchange factors: An integrated regulatory and functional view. *Small GTPases* 5(2):9.
7. Crespo P, Schuebel KE, Ostrom AA, Gutkind JS, Bustelo XR (1997) Phosphotyrosine-dependent activation of Rac-1 GDP/GTP exchange by the vav proto-oncogene product. *Nature* 385(6612):169–172.
8. Tybulewicz VL (2005) Vav-family proteins in T-cell signalling. *Curr Opin Immunol* 17(3):267–274.
9. Wu J, Katzav S, Weiss A (1995) A functional T-cell receptor signaling pathway is required for p95vav activity. *Mol Cell Biol* 15(8):4337–4346.
10. Kuhne MR, Ku G, Weiss A (2000) A guanine nucleotide exchange factor-independent function of Vav1 in transcriptional activation. *J Biol Chem* 275(3):2185–2190.
11. Zhou Z, et al. (2007) The calponin homology domain of Vav1 associates with calmodulin and is prerequisite to T cell antigen receptor-induced calcium release in Jurkat T lymphocytes. *J Biol Chem* 282(32):23737–23744.
12. Saveliev A, et al. (2009) Function of the nucleotide exchange activity of Vav1 in T cell development and activation. *Sci Signal* 2(101):ra83.
13. Reynolds LF, et al. (2002) Vav1 transduces T cell receptor signals to the activation of phospholipase C-gamma1 via phosphoinositide 3-kinase-dependent and -independent pathways. *J Exp Med* 195(9):1103–1114.
14. Barreira M, et al. (2014) The C-terminal SH3 domain contributes to the intramolecular inhibition of Vav family proteins. *Sci Signal* 7(321):ra35.
15. Yu B, et al. (2010) Structural and energetic mechanisms of cooperative autoinhibition and activation of Vav1. *Cell* 140(2):246–256.
16. Turner M, et al. (1997) A requirement for the Rho-family GTP exchange factor Vav in positive and negative selection of thymocytes. *Immunity* 7(4):451–460.
17. Kong YY, et al. (1998) Vav regulates peptide-specific apoptosis in thymocytes. *J Exp Med* 188(11):2099–2111.
18. Fischer KD, et al. (1998) Vav is a regulator of cytoskeletal reorganization mediated by the T-cell receptor. *Curr Biol* 8(10):554–562.
19. Costello PS, et al. (1999) The Rho-family GTP exchange factor Vav is a critical transducer of T cell receptor signals to the calcium, ERK, and NF-kappaB pathways. *Proc Natl Acad Sci USA* 96(6):3035–3040.
20. Holsinger LJ, et al. (1998) Defects in actin-cap formation in Vav-deficient mice implicate an actin requirement for lymphocyte signal transduction. *Curr Biol* 8(10):563–572.
21. Reynolds LF, et al. (2004) Vav1 transduces T cell receptor signals to the activation of the Ras/ERK pathway via LAT, Sos, and RasGRP1. *J Biol Chem* 279(18):18239–18246.
22. Tarakhovsky A, et al. (1995) Defective antigen receptor-mediated proliferation of B and T cells in the absence of Vav. *Nature* 374(6521):467–470.
23. Zhang R, Alt FW, Davidson L, Orkin SH, Swat W (1995) Defective signalling through the T- and B-cell antigen receptors in lymphoid cells lacking the vav proto-oncogene. *Nature* 374(6521):470–473.
24. Cao Y, et al. (2002) Pleiotropic defects in TCR signaling in a Vav-1-null Jurkat T-cell line. *EMBO J* 21(18):4809–4819.
25. Palomero T, et al. (2014) Recurrent mutations in epigenetic regulators, RHOA and FYN kinase in peripheral T cell lymphomas. *Nat Genet* 46(2):166–170.
26. Yoo HY, et al. (2014) A recurrent inactivating mutation in RHOA GTPase in angioimmunoblastic T cell lymphoma. *Nat Genet* 46(4):371–375.
27. Crescenzo R, et al.; European T-Cell Lymphoma Study Group, T-Cell Project: Prospective Collection of Data in Patients with Peripheral T-Cell Lymphoma and the AIRC 5xMille Consortium "Genetics-Driven Targeted Management of Lymphoid Malignancies" (2015) Convergent mutations and kinase fusions lead to oncogenic STAT3 activation in anaplastic large cell lymphoma. *Cancer Cell* 27(4):516–532.
28. Sakata-Yanagimoto M, et al. (2014) Somatic RHOA mutation in angioimmunoblastic T cell lymphoma. *Nat Genet* 46(2):171–175.
29. Fairbrother WG, Chasin LA (2000) Human genomic sequences that inhibit splicing. *Mol Cell Biol* 20(18):6816–6825.
30. Katzav S, Martin-Zanca D, Barbacid M (1989) vav, a novel human oncogene derived from a locus ubiquitously expressed in hematopoietic cells. *EMBO J* 8(8):2283–2290.
31. Katzav S, Cleveland JL, Heslop HE, Pulido D (1991) Loss of the amino-terminal helix-loop-helix domain of the vav proto-oncogene activates its transforming potential. *Mol Cell Biol* 11(4):1912–1920.
32. Katzav S (2015) Vav1: A Dr. Jekyll and Mr. Hyde protein—Good for the hematopoietic system, bad for cancer. *Oncotarget* 6(30):28731–28742.
33. Kataoka K, et al. (2015) Integrated molecular analysis of adult T cell leukemia/lymphoma. *Nat Genet* 47(11):1304–1315.
34. Boddicker RL, et al. (2016) Integrated mate-pair and RNA sequencing identifies novel, targetable gene fusions in peripheral T-cell lymphoma. *Blood* 128(9):1234–1245.
35. Dumont C, et al. (2009) Rac GTPases play critical roles in early T-cell development. *Blood* 113(17):3990–3998.
36. Ruiz S, Santos E, Bustelo XR (2009) The use of knockout mice reveals a synergistic role of the Vav1 and Rasgrf2 gene deficiencies in lymphomagenesis and metastasis. *PLoS One* 4(12):e8229.
37. Oberley MJ, Wang DS, Yang DT (2012) Vav1 in hematologic neoplasms, a mini review. *Am J Blood Res* 2(1):1–8.
38. Eckert RL, Lee KC (2006) S100A7 (psoriasin): A story of mice and men. *J Invest Dermatol* 126(7):1442–1444.
39. Crozet F, et al. (1997) Cloning of the genes encoding two murine and human cochlear unconventional type I myosins. *Genomics* 40(2):332–341.
40. Bianchetti CM, Blouin GC, Bitto E, Olson JS, Phillips GN, Jr (2010) The structure and NO binding properties of the nitrophorin-like heme-binding protein from *Arabidopsis thaliana* gene locus At1g79260.1. *Proteins* 78(4):917–931.
41. Diederichs S, et al. (2016) The dark matter of the cancer genome: Aberrations in regulatory elements, untranslated regions, splice sites, non-coding RNA and synonymous mutations. *EMBO Mol Med* 8(5):442–457.
42. Kong-Beltran M, et al. (2006) Somatic mutations lead to an oncogenic deletion of Met in lung cancer. *Cancer Res* 66(1):283–289.
43. Puente XS, et al. (2015) Non-coding recurrent mutations in chronic lymphocytic leukaemia. *Nature* 526(7574):519–524.
44. Trifonov V, Pasqualucci L, Tiacci E, Falini B, Rabadan R (2013) SAVI: A statistical algorithm for variant frequency identification. *BMC Syst Biol* 7(Suppl 2):S2.
45. McKenna A, et al. (2010) The Genome Analysis Toolkit: A MapReduce framework for analyzing next-generation DNA sequencing data. *Genome Res* 20:1297–1303.
46. Narasimhan V, et al. (2016) BCFtools/RoH: a hidden Markov model approach for detecting autozygosity from next-generation sequencing data. *Bioinformatics* 32(11):1749–1751.
47. Iyer MK, Chinnaiyan AM, Maher CA (2011) ChimeraScan: A tool for identifying chimeric transcription in sequencing data. *Bioinformatics* 27(20):2903–2904.
48. Abate F, et al. (2014) Pegasus: A comprehensive annotation and prediction tool for detection of driver gene fusions in cancer. *BMC Syst Biol* 8:97.
49. Zugaza JL, et al. (2002) Structural determinants for the biological activity of Vav proteins. *J Biol Chem* 277(47):45377–45392.